- Technical Paper -

CRACKING RISK EVALUATION ON CONTINUOUS REINFORCED CONCRETE PAVEMENT WITH SUPPLEMENTARY CEMENTITIOUS MATERIALS AND EXPANSIVE ADDITIVE

Hyo Eun JOO[*1], Tomoki NAGATA[*2] and Yuya TAKAHASHI [*3]

ABSTRACT

This study aims to evaluate the cracking risk of continuous reinforced concrete pavement (CRCP) under various mix conditions including supplementary cementitious materials (SCMs) and expansive additives (EA). A multiscale chemo-hygral computational analysis was utilized and the model was validated using strain data from lab-scale concrete and full-scale CRCP specimens. The analysis model accurately reproduced the strain behaviors in CRCP with SCMs and EA, and the analysis results showed that the amount of EA significantly reduces the risk of cracking.

Keywords: continuous reinforced concrete pavement, expansive additive, fly ash, cracking risk

1. INTRODUCTION

Continuous reinforced concrete pavement (CRCP) controls cracks not through the joints, but the reinforcing bars placed continuously [1,2]. Because the concrete pavements with joints are designed to induce cracks at specific locations, this can result in concentrated damage at the joints, leading to a rapid deterioration in the concrete durability [3,4]. In contrast, CRCP system ensures higher durability by inducing small and evenly distributed cracks.

Meanwhile, supplementary cementitious materials (SCMs), such as fly ash (FA) and blast furnace slag (BFS), are increasingly recommended due to their benefits in reducing carbon dioxide emissions and enhancing the long-term durability of concrete structures. However, SCMs tends to reduce cracking resistance of concrete compared to ordinary Portland cement (OPC) [5,6]. To mitigate the increased cracking risk in CRCP under drying condition, the use of expansive additives (EA) can be considered, as they induce initial expansion to compensate for the shrinkage [7,8].

However, there is a lack of previous research on the cracking risk of CRCP with SCMs and EA; therefore, this study aims to assess the cracking risk of CRCP with various mix proportions by utilizing a multiscale chemo-hygral computational analytical system (DuCOM-COM3) [9]. The EA model [7,10] in analytical system was validated in this study, by using the strains measured from lab-scale concrete and full-scale CRCP specimens [11]. Based on the analysis results, the cracking risk of CRCP was also evaluated, and the effect of several parameters on the cracking risk were analytically investigated.

2. METHODOLOFY FOR CRACKING RISK EVALUATION

2.1 Overview of numerical system

This study utilizes the multiscale chemo-hygral computational system, DuCOM-COM3 [9]. This system is capable of simulating the thermodynamic and mechanical behaviors of concrete based on a finite element model, considering cement hydration, pore structure development, and moisture transport. This analysis model has an advantage in that it can simulate the initial expansion of concrete induced by EA, reflecting internal pressure generated by hydrates of EA phase. The effect of restraint on the expansion was reflected through anisotropic pressure that caused by EA in the poromechanical model, and the modelling details and its validity can be found elsewhere [7,10].

2.2 Target experiments and numerical conditions

The experiments conducted by Kurebayashi et al. [11] are utilized for model validations in this study. In the experiment, the concrete prism specimens without reinforcement with dimensions of 20cm×20cm×80 cm and real-scale CRCP specimens with a length of 40 m, width of 3.5 m, and depth of 25 cm (Fig. 1) were manufactured to observe the strain behaviors at Nihon University, Fukushima Prefecture. As shown in Table 1, each test specimen had three mixing cases, i.e., OPC case, FA+EA case (OPC replaced by FA with EA), and BB+EA case (BFS cement with EA), and the mix proportions are shown in Table 2. Water to binder ratio (W/B) were 40.1, 34.9, and 40.1 % in OPC, FA+EA, and BB+EA, respectively.

*1 Postdoctoral researcher, Dept. of Civil Engineering, The University of Tokyo, Dr.E., JCI Member
*2 Graduate School of Engineering, The University of Tokyo, JCI Student Member
*3 Associate Professor, Dept. of Civil Engineering, The University of Tokyo, Dr.E., JCI Member

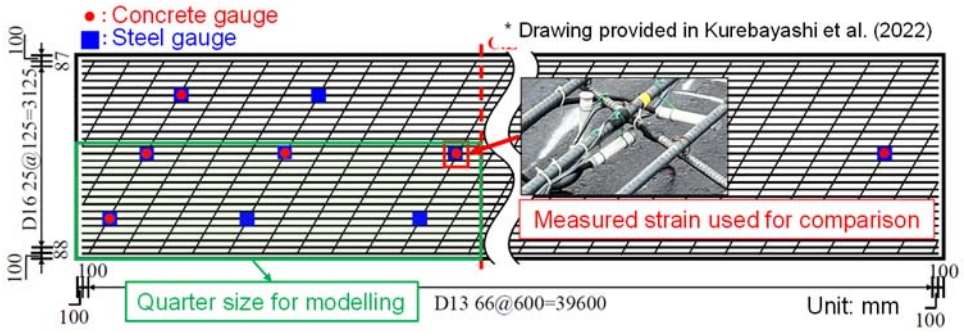

Fig. 1 Drawing of CRCP specimen [10]

Table 1 Specimen lists of experiment

Specimens	Mix proportion	Reinforced
Concrete prism	OPC FA+EA BB+EA	No
Full-scale CRCP	OPC FA+EA BB+EA	Yes

Table 2 Mix proportion (Unit: [kg/m^3])

Mix ID	W	C	FA	BFS	EA	S	G
OPC	162	404	0	0	0	602	1193
FA+EA	162	363	81	0	20	507	1129
BB+EA	162	202	0	182	20	592	1173

For the EA, HYPER EXPAN-K, produced by Taiheiyo Company in Japan, was used.

For numerical investigation, meshes for the lab-scale specimens and real-scale CRCP specimens were made as shown in Figs 2 and 3. For lab-scale specimens, the first 7 days were wet curing period, and therefore the relative humidity (RH) was set to be 100% in the analysis. Heat and moisture transfer from the air into concrete was allowed on all surfaces exposed to the air. The strain measured at the center of specimens for 28 days was compared with the analysis results. For real-scale CRCP, the strains in the x, y, and z directions measured at the center area marked in Fig. 1 were compared with those obtained from the simulation. All the concrete strains in x, y and z directions were measured at the depth of reinforcing bars. The x-direction is the longitudinal direction, the y-direction is the transverse direction, and the z-direction is the vertical direction. To reduce the computational time, a quarter of CRCP specimen was modelled; thus, the analysis model has 20 m in length and 1.75 m in width, and fixed boundary conditions were applied to the symmetric surface. Under the CRCP, asphalt with a depth of 4 cm, cement layers with a depth of 20 cm, and soil layers with a depth of 500 cm were modeled using elastic elements. The elastic moduli of the asphalt, cement, and soil layers were 1000, 3000, and 80 MPa, with Poisson's ratios of 0.35, 0.2, and 0.35, respectively. In the CRCP elements, as the reinforcing bars were arranged in x- and y-directions with 0.56% and 0.6% reinforcement ratios, respectively, reinforced concrete (RC) elements were used, as colored with red color in Fig. 3(b). The layers colored with blue represent plain concrete elements without reinforcement. The mechanical properties of

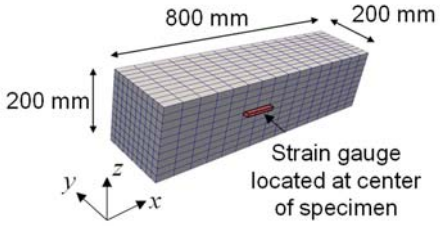

Fig. 2 Meshes for lab-scale specimen

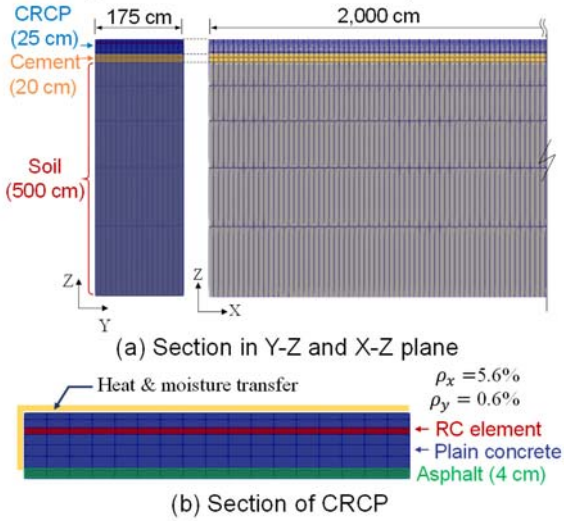

Fig. 3 Analytical meshes for CRCP

the concrete were determined by hydration analysis in the DuCOM-COM3 system, and the elastic modulus and yield strength of the reinforcement were 21 GPa and 400 MPa, respectively. Heat and moisture transfer was allowed through the upper and side surfaces of the CRCP elements. The temperature and humidity conditions were input based on weather data from October 2022 reported by the Meteorological Administration of Japan (Fig. 4).

2.3 Method for cracking risk evaluation

According to the JSCE standard specifications for concrete structures [12], the probability of cracking can be estimated using the cracking index [$I_{cr}(t)$], which can be determined according to time (t) as follows:

$$I_{cr} = f_t / \sigma_{conc} \quad (1)$$

where,

f_t : Tensile strength of concrete

σ_{conc} : Maximum concrete stress

where f_t is the tensile strength of concrete, and σ_{conc} is the maximum stress of concrete. σ_{conc} can be obtained from the analysis. The cracking index should be designed to be less than the safety factor to control the probability of cracking, as shown in Fig. 5; thus, the probability of cracking increases as the cracking index decreases.

3. MODEL VALIDATION

3.1 Lab-scale concrete specimens

In Fig. 6, the temperature of concrete derived from analysis is compared with that measured in the experiment at the center of the specimens. The internal heat of concrete calculated from the computational system takes into account hydration process according to different mix proportions and thermal transfer between the exposed environment and concrete. Through the analysis results, it was confirmed that the hydration and heat transfer models can properly reproduce the internal heat of concrete with different mix proportions.

Fig.7 compares the strain of concrete measured in the experiment with that derived from the analysis. In OPC case without EA, the largest drying shrinkage occurred at about -300 με over 28 days, which was well reproduced by the analysis model. For the cases where EA was incorporated, the expansion caused by temperature change was removed from the strain derived from analysis and experiment by Eq. (2), in order to verify whether the analytical model properly reflect the effect of EA.

$$\varepsilon_{x,T=20℃} = \varepsilon_x + C\cdot(20℃ - T) \quad (2)$$

where,

ε_x : strain calculated at T

C : thermal strain of concrete (=10με/℃)

As shown in Fig. 7(b), for FA+EA case, the analysis model was found to well reproduce the initial expansion and shrinkage strain. For BB+EA case, however, there was a discrepancy between the experimental and analytical results (refer to 'Analysis (EA20)' in Fig. 7(c)). This is because the analysis model does not properly reflect the reaction mechanism when BFS cement and EA are incorporated

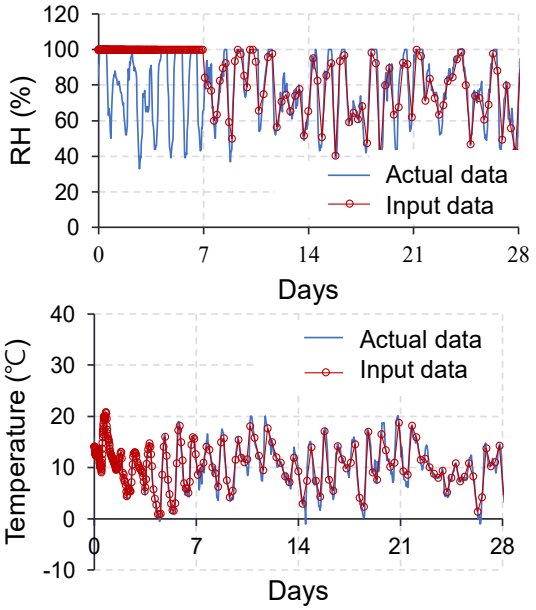

Fig. 4 Environmental data

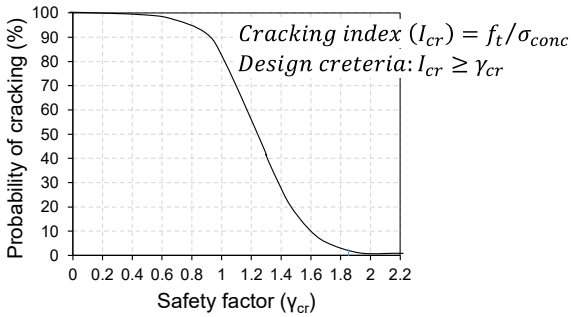

Fig. 5 Cracking probability − safety factor [11]

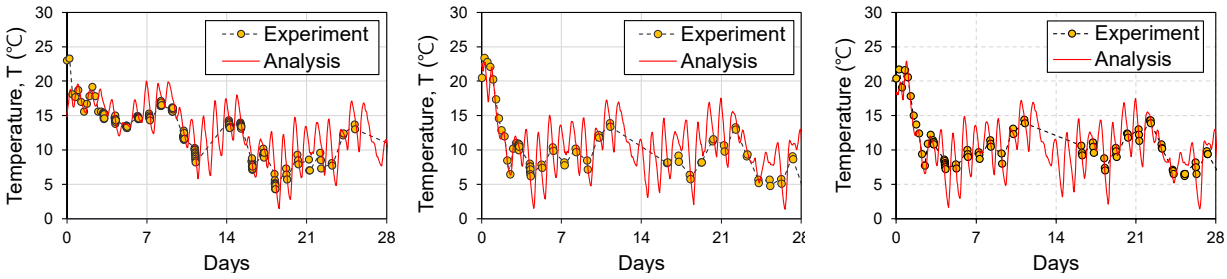

Fig. 6 Comparison of temperatures with lab-scale concrete specimens

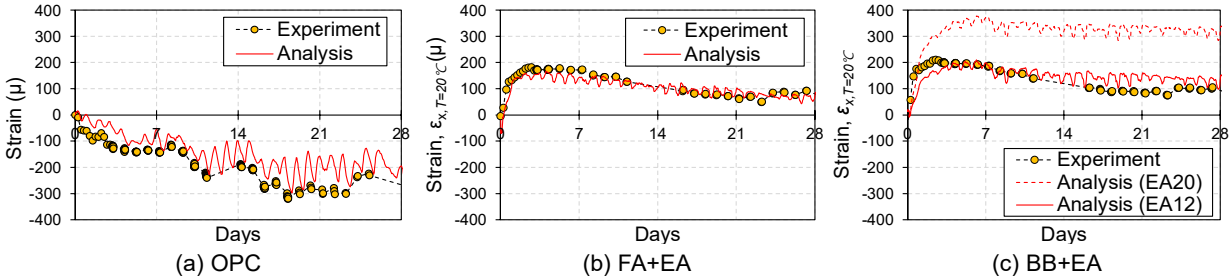

Fig. 7 Comparison of strain behaviors with lab-scale concrete specimens

together. Thus, for the case of BB+EA, the amount of EA required to reproduce the free expansion observed in experiments was determined through calibration. The results showed that the analysis model closely predicted the expansion of the specimen when 12 kg/m^3 of EA was incorporated (see 'Analysis (EA 12)' in Fig. 5(c)). The model improvements are necessary in future, considering the reaction mechanism in BFS cement and EA. However, the primary objective of this study was to analyze the behavior of full-scale CRCP based on the strains of lab-scale specimens. Therefore, the EA amount derived through calibration was applied in the analysis of full-scale CRCP.

3.2 Full-scale CRCP specimens

The strains in x, y, and z-directions measured in the experiment were compared with the analysis results, as shown in Fig. 8, where the yellow lines denote the test data, and the red lines represent the analysis results. In OPC case without EA, significant drying shrinkage occurred, and the shrinkage was smallest in the x-direction which had a higher reinforcement ratio compared to other directions. FA+EA and BB+EA cases showed the anisotropic expansion due to EA, as presented in Figs.8 (b) and (c). The strain in x direction was significantly smaller than those in y and z directions because of higher reinforcement ratio and restrictions by substructures (i.e., asphalt, cement, and soil layers) due to longer length in x direction. The analytical model accurately assessed the reduction in drying shrinkage due to the incorporation of EA and well reproduced the anisotropic strain behavior.

Fig. 9 shows the principal strain distribution obtained from the analysis results at 120 days. In FA+EA case, the tensile stain is slightly concentrated on the surface compared to other cases; however, severe crack propagation in the concrete was not observed in all three mix proportions under the given condition.

4. CRCKING RISK EVALUATION ON CRCP

4.1 Cracking risks of CRCP specimens

Fig. 10 represents the stress distribution of concrete in x-direction and the tensile strength of concrete. Note that the stress is taken as the average value of the stresses of three concrete elements between the RC and asphalt elements. Fig. 11 shows the cracking index calculated according to JSCE guidelines, based on the stress and tensile strength of concrete presented in Fig. 10. In FA+EA, the initial concrete stresses were higher than those in other cases. This is because the change in strain due to the initial temperature change inside the concrete was greatest in FA+EA case (see Fig. 8). In addition, the cases with EA showed a slightly higher cracking index than OPC case; however, the cracking indices in all cases calculated at 120 days were similar, and the risks was in the range from 0% to 5%. This implies that the FA+EA and BB+EA cases ensure the cracking risk comparable to the OPC case by using EA.

4.2 Cracking risk evaluation in various conditions

In the actual construction of CRCPs, the parameters affecting the cracking risk, such as the amount of EA and elastic modulus of substructures (i.e., asphalt), can be changed from those in the target experiment. Thus, based on the validated analysis model, further investigations were conducted on FA+EA case, which is the target mixing proportion applied for actual construction site in future study.

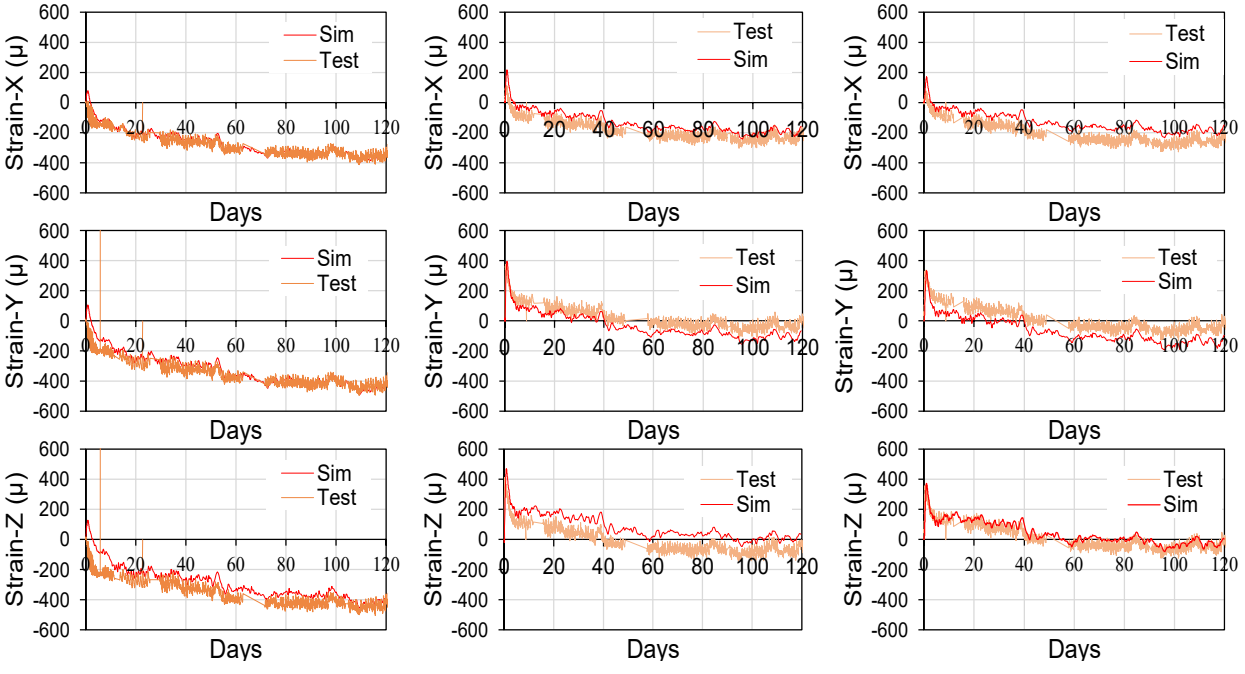

(a) OPC (b) FA+EA (c) BB+EA

Fig. 8 Comparison of strain behaviors with full-scale CRCP specimens

Here, the effect of EA content in the mix proportion and the effect of elastic modulus of asphalt layer is studied. First, in Fig. 12, '0.5 EA' refers to a mix proportions with 3% of the EA amount used in FA+EA case, while 'no EA' refers to a mix without any EA admixture. According to the analysis results, the cracking risk was found to increase from 3% to 92% as the amount of EA decreased (Table 3). Fig. 13 shows the effect of the elastic modulus of the asphalt, a substructural material, on the cracking risk. The elastic modulus of asphalt of 1000 and 30000 MPa were used in the analysis considering that it changes depending on the environmental temperature [13]. It was observed that the elastic modulus of the asphalt has minimal influence on the cracking risk under the given environmental conditions.

Through this study, the applicability of the analytical EA model implemented in DuCOM-COM3 was verified in real-scale RC structures. Therefore, it is expected to contribute to developing a time-dependent risk assessment system for structures under natural environment. Furthermore, a more advanced

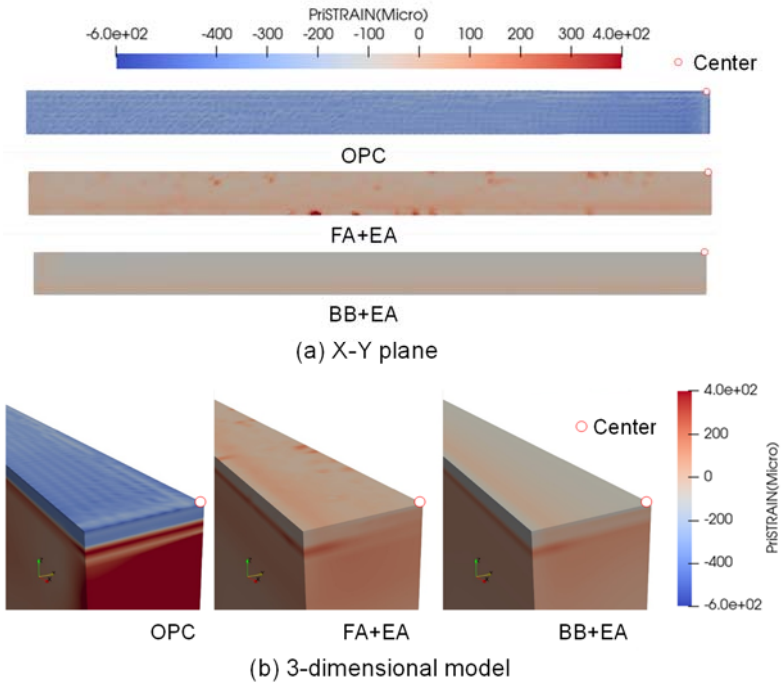

Fig. 9 Simulated principal strain distribution

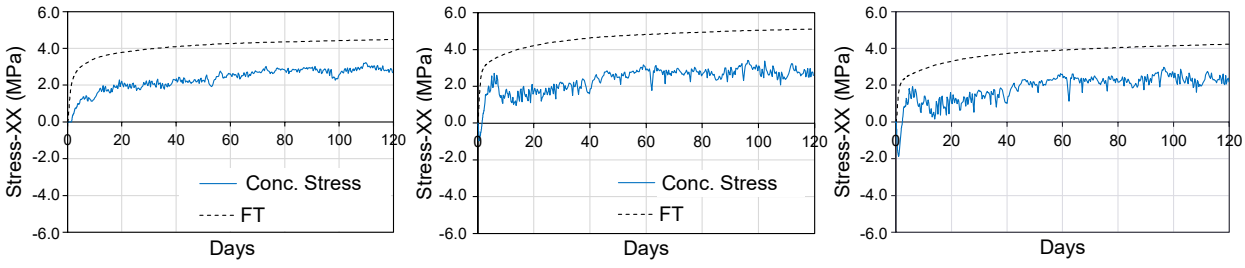

Fig. 10 Simulated concrete stress distibution at full-scale CRCP specimens

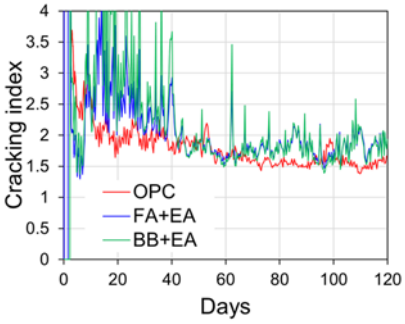

Fig. 11 Crackikng risk evluation

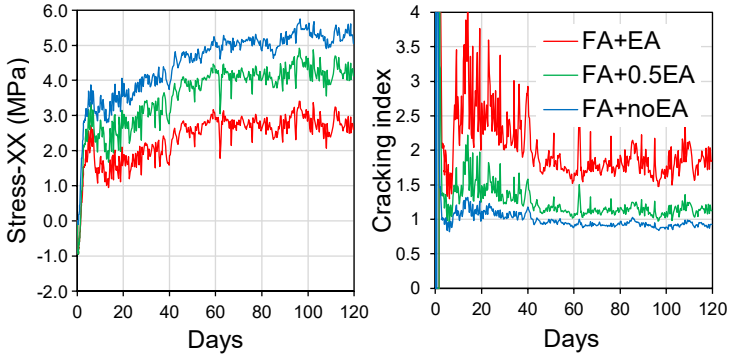

Fig. 12 Effect of EA on cracking risk

Table 3 Effect of EA on cracking risk

Case	Index	Risk
FA + EA	1.85	3%
FA + 0.5EA	1.12	70%
FA + noEA	0.85	92%

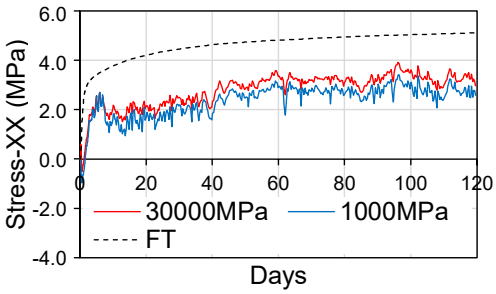

Fig. 13 Effect of elastic modulus of asphalt on cracking

assessment of risk considering the combined effects of chloride ion penetration and fatigue loading will be performed in future research.

5. Conclusions

The cracking risk of CRCP incorporating SCMs and EA was evaluated based on the numerical analysis. The analysis results showed that the CRCP, where SCMs replaced by OPC and EA was incorporated, had the same level of cracking risk as that with only OPC. This implies that the FA+EA and BB+EA cases ensure the cracking risk comparable to the OPC case by using EA. In addition, it was confirmed that increasing the amount of EA can significantly reduce the cracking risk, suggesting that adjusting EA amount can enhance the durability of CRCP.

AKCKNOWLEDGEMENT

This research was conducted under the "Technical Research and Development on Highly Durable Fly Ash Concrete Pavements Based on Data Assimilation" commissioned by the Ministry of Land, Infrastructure, Transport and Tourism (MLIT) under the Technical Research and Development Program of the New Road Technology Council established by the Road Bureau of MLIT. We are thankful to Prof. Ichiro Iwaki and Dr. Takuya Maeshima from Nihon University for their advice for CRCP analyses.

REFERENCES

[1] Roesler, J. R., Hiller, J. E., and Brand, A. S., "Continuously Reinforced Concrete Pavement Manual, Guidelines for Design, Construction, Maintenance, and Rehabilitation Report FHWA-HIF-16-026", Aug. 2016.

[2] Shi, X., Zollinger, D. G., and Mukhopadhyay, A. K., "Punchout Study for Continuously Reinforced Concrete Pavement containing Reclaimed Asphalt Pavement using Pavement ME Models", Int. J. Pavement Eng., Vol. 21, pp. 1199–1212, Aug. 2020.

[3] Suraneni, P., Burkan Isgor, O., and Weiss, W. J., "Deicing Salts and Durability of Concrete Pavements and Joints: Mitigating Calcium Oxychloride Formation", ACI Concr. Int., Vol. 38, No. 4, pp. 48–54, Apr. 2016.

[4] Lu, L., Zhao, D., Fan, J., and Li, G., "A brief review of sealants for cement concrete pavement joints and cracks", Road Mater. and Pavement Design, Vol. 23, No. 7, pp. 1467–1491, Jul. 2022.

[5] Suntharalingam, S., and Takahashi, Y., "Experimental study on autogenous shrinkage behaviors of different Portland blast furnace slag cements", Constr. Build. Mater., Vol. 230, p. 116980, Jan. 2020.

[6] Wang, L., Yu, Z., Liu, B., Zhao, F., Tang, S., and Jin, M., "Effects of Fly Ash Dosage on Shrinkage, Crack Resistance and Fractal Characteristics of Face Slab Concrete", Fractal and Fractional, Vol. 66, No. 335, June 2022.

[7] Kolneath, P., "Thermodynamic Modeling of Expansive Additives in Reinforced Concrete", Ph.D. thesis, The Univ. of Tokyo, Tokyo, Japan, 2020.

[8] Tran, N. P., Gunasekara, C., Law, D. W., Houshyar, S., Setunge, S., and Cwirzen, A., "A Critical Review on Drying Shrinkage Mitigation Strategies in Cement-based Materials", J. Build. Eng., Vol. 38, p. 102210, Jun. 2021.

[9] Maekawa, K., Ishida, T., and Kishi, T., "Multi-scale Modeling of Struct. Concr.", OX: Taylor & Francis, 2008.

[10] Gupta, M., "Study on mechanical properties and multiscale expansion modelling for concrete with expansive additives under different restraint conditions using Poro-mechanics", Ph.D. thesis, The University of Tokyo, Tokyo, Japan, 2022.

[11] Kurebayashi, K., Shiratori, T., Kanno, H., He, Z., Maeshima, T., and Iwaki, I., "Experimental study on expansion and shrinkage behavior of continuous reinforced concrete pavement with various admixtures", in Proc. Tech. Res. Pres. Meet. JSCE Tohoku Branch, Vol.10, Fukushima, Japan: Nihon Univ., 2022.

[12] Japanese Society of Civil Engineers, "Standard Specifications for Concrete Structures-2007 'Design'", Tokyo, Japan: JSCE 2010 Concrete Committee, 2010.

[13] Saito, Y., Maeshima, T., Watanabe, S., Naito, H., Iwaki, I., "Basic Study on Evaluation Method of Damage Degree of Asphalt Pavement by Local Vibration Test (In Japanese)", Proceedings of the 27th Symposium on Pavement Engineering, No. PL2022-041, 2022.